THE JOURNAL OF BIOLOGICAL CHEMISTRY VOL. 280, NO. 37, pp. 32362–32371, September 16, 2005

Deletion of Cg-*emb* in Corynebacterianeae Leads to a Novel Truncated Cell Wall Arabinogalactan, whereas Inactivation of Cg-*ubiA* Results in an Arabinan-deficient Mutant with a Cell Wall Galactan Core*

Received for publication, June 10, 2005 Published, JBC Papers in Press, July 21, 2005, DOI 10.1074/jbc.M506339200

Luke J. Alderwick[‡1], Eva Radmacher[§2], Mathias Seidel[§2], Roland Gande[§2], Paul G. Hitchen[¶‖], Howard R. Morris[¶‖3], Anne Dell[¶3,4], Hermann Sahm[§2], Lothar Eggeling[§2], and Gurdyal S. Besra[‡5]

From the [‡]School of Biosciences, University of Birmingham, Edgbaston, Birmingham B15 2TT, United Kingdom, the [§]Institute for Biotechnologie 1, Research Centre Juelich, D-52425 Juelich, Germany, the [¶]Division of Molecular Biosciences, Faculty of Life Sciences, Imperial College, London SW7 2AZ, United Kingdom, and [‖]M-SCAN Mass Spectrometry Research and Training Centre, Silwood Park, Ascot SL5 7PZ, United Kingdom

The cell wall of *Mycobacterium tuberculosis* has a complex ultrastructure that consists of mycolic acids connected to peptidoglycan via arabinogalactan (AG) and abbreviated as the mAGP complex. The mAGP complex is crucial for the survival and pathogenicity of *M. tuberculosis* and is the target of several anti-tubercular agents. Apart from sharing a similar mAGP and the availability of the complete genome sequence, *Corynebacterium glutamicum* has proven useful in the study of orthologous *M. tuberculosis* genes essential for viability. Here we examined the effects of particular genes involved in AG polymerization by gene deletion in *C. glutamicum*. The anti-tuberculosis drug ethambutol is thought to target a set of arabinofuranosyltransferases (Emb) that are involved in arabinan polymerization. Deletion of *emb* in *C. glutamicum* results in a slow growing mutant with profound morphological changes. Chemical analysis revealed a dramatic reduction of arabinose resulting in a novel truncated AG structure possessing only terminal arabinofuranoside (t-Ara*f*) residues with a corresponding loss of cell wall bound mycolic acids. Treatment of wild-type *C. glutamicum* with ethambutol and subsequent cell wall analyses resulted in an identical phenotype comparable to the *C. glutamicum emb* deletion mutant. Additionally, disruption of *ubiA* in *C. glutamicum*, the first enzyme involved in the biosynthesis of the sugar donor decaprenol phosphoarabinose (DPA), resulted in a complete loss of cell wall arabinan. Herein, we establish for the first time, (i) that in contrast to *M. tuberculosis embA* and *embB* mutants, deletion of *C. glutamicum emb* leads to a highly truncated AG possessing t-Ara*f* residues, (ii) the exact site of attachment of arabinan chains in AG, and (iii) DPA is the only Ara*f* sugar donor in AG biosynthesis suggesting the presence of a novel enzyme responsible for "priming" the galactan domain for further elaboration by Emb, resulting in the final maturation of the native AG polysaccharide.

The Corynebacterianeae represent a distinct and unusual group within Gram-positive bacteria, with the most prominent members being the human pathogens *Mycobacterium tuberculosis* and *Mycobacterium leprae* (1). In addition, the human pathogen *Corynebacterium diphtheriae* is the causal agent of diphtheria, and serious economic losses occur from the infection of animals by corynebacterial strains, such as *Corynebacterium pseudotuberculosis* and *Corynebacterium matruchotii* (2, 3). Furthermore, non-pathogenic bacteria belong to this taxon, such as *Corynebacterium glutamicum*, which is used in the industrial production of amino acids (4). A common feature to all these bacteria is that they possess an unusual cell wall matrix composed of mycolic acids, arabinogalactan, and peptidoglycan and is often referred to as the mycolyl-arabinogalactan-peptidoglycan (mAGP)[6] complex (5–9).

Arabinogalactan (AG) plays a crucial role in covalently anchoring the outer lipid layer to peptidoglycan. Synthesis of AG begins with the formation of the linker unit through the transfer of GlcNAc-1-P and Rha from their respective sugar nucleotides (UDP-GlcNAc and dTDP-Rha) to form polyprenol-P-P-GlcNAc and polyprenol-P-P-GlcNAc-Rha lipid intermediates (10, 11). The intermediates polyprenol-P-P-GlcNAc and polyprenol-P-P-GlcNAc-Rha then serve as acceptors for the sequential addition of galactofuranose (Gal*f*) residues from UDP-Gal*f* (generated from UDP-Gal*p* via Glf (12, 13)) to form polyprenol-P-P-GlcNAc-Rha-Gal_{30} through a novel enzyme designated GlfT (Rv3808c). This latter enzyme expresses two glycosyltransferase activities, a UDP-Gal*f*:β-D-(1→5)-Gal*f* and a UDP-Gal*f*:β-D-(1→6)-Gal*f*, both activities being required for alternating β(1→5) and β(1→6) linkages during galactan polymerization (11, 14). Chemical analysis of the mature lipid-linked galactan, synthesized *in vitro* (11), suggests that this intermediate then serves as the acceptor for the subsequent addition of arabinofuranose (Ara*f*) residues from the arabinose sugar donor β-D-arabinofuranosyl-1-monophosphoryldecaprenol (DPA) in the formation of the Ara*f* portion (α1→5, α1→3, and β1→2 linkages) of AG (15–18). The AG-lipid intermediate at some point is mycolylated and transglycosylated to peptidoglycan (19, 20).

Early studies demonstrated that administration of ethambutol (EMB) led to a rapid cessation of mycolic acid transfer to the cell wall and an

* The costs of publication of this article were defrayed in part by the payment of page charges. This article must therefore be hereby marked "*advertisement*" in accordance with 18 U.S.C. Section 1734 solely to indicate this fact.
[1] Supported by a Biotechnology and Biological Sciences Research Council (BBSRC) quota studentship.
[2] Supported by a Degussa grant (Düsseldorf, Germany).
[3] Supported by grants from the BBSRC and the Wellcome Trust.
[4] A BBSRC Professorial Research Fellow.
[5] Supported by a Lister Institute-Jenner Research Fellowship and the Medical Research Council, UK. To whom correspondence should be addressed. Tel.: 44-121-415-8125; Fax: 44-121-414-5925; E-mail: g.besra@bham.ac.uk.

[6] The abbreviations used are: mAGP, mycolyl arabinogalactan peptidoglycan; AG, arabinogalactan; Ara, arabinose; CMAME, corynomycolic acid methyl ester; DPA, decaprenol phosphoarabinose; EMB, ethambutol; Gal, galactose; GC, gas chromatography; GC/MS, gas chromatography/mass spectrometry; GlcNAc, *N*-acetyl-galactosamine; MALDI-TOF, matrix-assisted laser desorption/ionization time-of-flight; Rha, rhamnose; OD, optimal density.

accumulation of trehalose monomycolate and trehalose dimycolate (21). Subsequently, EMB was shown to inhibit specifically AG biosynthesis (22). The precise molecular target of EMB occupies the *emb* locus in *Mycobacterium avium* and *M. tuberculosis*. The locus consists of *embRAB* in *M. avium* (23) and *embCAB* in *M. tuberculosis* (24). To further define the role of EmbCAB proteins in arabinan biosynthesis, *embA*, *embB*, and *embC* genes were inactivated individually in *Mycobacterium smegmatis* (25, 26). Although all three mutants were viable, only the crucial terminal Ara_6 motif, which is the template for mycolylation in AG, was altered in both *embA* and *embB* mutants with the remaining AG structure intact (25). This suggested that both EmbA and EmbB are involved in the formation of the terminal Ara_6 motif in AG, and EmbC in the formation of arabinan in lipoarabinomannan (26). Our preliminary attempts to obtain deletion mutants of *embA* and *embB* in *M. tuberculosis* or *embAB* in *M. smegmatis* have proved unsuccessful,[7] presumably due to the essentiality of cell wall mAGP (27–29).

In the present study we have established through comparative genomic analyses the first biochemical and molecular description of compete ablation of cell wall arabinan biosynthesis in a non-mycobacterial spp., and we highlight the inherent usefulness of examining related spp. to probe complex biosynthetic pathways.

MATERIALS AND METHODS

Strains and Culture Conditions—*C. glutamicum* ATCC 13032 (the wild-type strain, and referred for the remainder of the text as *C. glutamicum*) and *Escherichia coli DH5αmcr* were grown in Luria-Bertani (LB) broth (Difco) at 30 °C and 37 °C, respectively. The mutants generated in this study were grown on BHIS (5 g of Tryptone, 5 g of NaCl, 2.5 g of yeast extract, 18.5 g of brain heart infusion (Difco), and 90.1 g of sorbitol per liter). Kanamycin and ampicillin were used at a concentration of 50 μg/ml. The minimal medium CGXII was used for *C. glutamicum* (30). Samples for lipid analyses were prepared by harvesting cells at an optical density (OD) of 10–15, followed by a saline wash and freeze drying. Cultivation of *C. glutamicum*Δ*emb* for lipid and cell wall analysis required two pre-cultures: Firstly, a 5-ml BHIS culture was grown for 8 h, which was then used to inoculate a 50-ml BHIS culture for 15 h. This was then used to inoculate a 100-ml BHIS culture to OD 1, which was harvested after reaching an OD 3.

Construction of Plasmids—The vectors used for deletion and inactivation were as follows: pK19mobsacBΔ*emb* (*NCgl0184*, *embC*), pCg::*ubiA* (*NCgl2781*, *Rv3806c*), with the gene numbers of the *C. glutamicum* and *M. tuberculosis* orthologs added in parentheses. The plasmid used for overexpression was pEKEx2*emb*. To enable deletion of gene cross-over PCR was applied to generate the fragments carrying fused sequences adjacent to the gene in question. The resulting fragments were ligated with pK19mobsacB, and the final plasmids were confirmed by sequencing. For *emb* deletion, the primers used were *emb*_start_in 5′-CCC ATC CAC TAA ACT TAA ACA CTC AAC TAC ATC TGA CAC GTT GAT C-3′, *emb*_start_out 5′-GCT TGG TGA GTT CGG AAA CAG GA-3′, *emb*_end_in 5′-TGT TTA AGT TTA GTG GAT GGG CTC TGG AAT CCA GGG CAT ATG AAG-3′, and *emb*_end_out 5′-TTC CAT GAG CAG CTG GCG ATA AC-3′. For the second PCR the primer pair *emb*_start_out and *emb*_end_out was used again. The resulting fragment was ligated with SmaI-cleaved pK19mobsacB to generate pK19mobsacBΔ*emb*. For inactivation of *ubiA* an internal fragment of 321 bp was amplified (p*ubiA*-for: ATC TTC AAC CAG CGC ACG ATC; p*ubiA*-rev: AAT ATC GAT CAC TGG CAT GTG C), which was made blunt and ligated into the SmaI site of the non-replicative vector pK18mob to yield pCg::*ubiA*.

Genomic Mutations—To enable chromosomal inactivation of *ubiA*, pCg::*ubiA* was introduced into *C. glutamicum* by electroporation. Selection for resistance to kanamycin yielded clones whose correct disruption of *ubiA* was confirmed with different primer pairs annealing in the vector and the bacterial chromosome.

Southern Blot Analysis—Genomic DNA was extracted from *C. glutamicum*Δ*emb* and the wild-type strain and cleaved with EcoRV. The resulting fragments were separated on a 1% agarose gel and blotted onto a Nytran NY13N nitrocellulose membrane, with subsequent washings according to standard protocols. Detection was carried out with a fragment generated by PCR with primers pEmbΔ1 (5′-GTG GTT TAG GGG GTC TGT TGG G-3′) and pEmbΔ2 (5′-GGC AGC GTG CCG ATC ATC GCC-3′) as probe that was labeled with digoxigenin (DIG labeling and detection kit, Roche Applied Science).

Extraction and Analysis of Cell Wall Bound Mycolic Acids from C. glutamicum Strains—Cells were grown as described above, harvested, washed, and freeze-dried. Cells (100 mg) were extracted by two consecutive extractions with 2 ml of $CHCl_3/CH_3OH/H_2O$ (10:10:3, v/v) for 3 h at 50 °C. The bound lipids from the delipidated extracts or purified cell walls (see below) were released by the addition of 2 ml of 5% aqueous solution of tetrabutylammonium hydroxide, followed by overnight incubation at 100 °C. After cooling, water (2 ml), CH_2Cl_2 (4 ml), and CH_3I (500 μl) were added and mixed thoroughly for 30 min. The lower organic phase was recovered following centrifugation and washed three times with water (4 ml), dried, and resuspended in diethyl ether (4 ml). After centrifugation the clear supernatant was again dried and resuspended in CH_2Cl_2 (100 μl). An aliquot (10 μl) from each strain was subjected to TLC using silica gel plates (5735 silica gel $60F_{254}$, Merck), and developed in petroleum ether/acetone (95:5, v/v) and charred using 5% molybdophosphoric acid in ethanol at 100 °C to reveal corynomycolic acid methyl esters (CMAMES) and compared with known standards (31).

Isolation of the mAGP Complex—The thawed bacterial cells were resuspended in phosphate-buffered saline containing 2% Triton X-100 (pH 7.2), disrupted by sonication and centrifuged at 27,000 − *g* (6, 7). The pelleted material was extracted three times with 2% SDS in phosphate-buffered saline at 95 °C for 1 h to remove associated proteins, successively washed with water, 80% (v/v) acetone in water, and acetone, and finally lyophilized to yield a highly purified cell wall preparation (6, 7).

Glycosyl Composition of Cell Walls by Alditol Acetates—Cell wall preparations were hydrolyzed in 250 μl of 2 M trifluoroacetic acid at 120 °C for 2 h as described (6, 7). Sugar residues were reduced with 50 μl of NaB^2H_4 (10 mg/ml in ethanol:1 M NH_3 (1:1)), and the resultant alditols were per-*O*-acetylated and examined by gas chromatography (GC) as described previously (6, 7).

Glycosyl Linkage Analysis of Cell Walls—Cell wall preparations (10 mg) were suspended in 0.5 ml of Me_2SO (anhydrous) and 100 μl of 4.8 M dimethyl sulfinyl carbanion (6, 7). The reaction mixture was stirred for 1 h, and then CH_3I was slowly added, and the suspension was stirred for a further 1 h; this process was repeated for a total of three times. The reaction mixture was then diluted with an equal volume of water, and the entire contents were dialyzed against water overnight. The resulting per-*O*-methylated cell wall samples were applied to a C_{18} Sep-Pak cartridge and purified as described previously (6, 7). The per-*O*-methylated cell walls were hydrolyzed using 250 μl of 2 M trifluoroacetic acid at 120 °C for 2 h. The resulting hydrolysate was reduced with NaB^2H_4, per-*O*-acetylated, and examined by gas chromatography/mass spectrometry (GC/MS) as described previously (6, 7).

Mass Spectrometry of Per-O-methylated Cell Walls—Per-*O*-methylated cell walls were prepared as described above. Methanolic-HCl was

[7] W. N. Maughan, unpublished results.

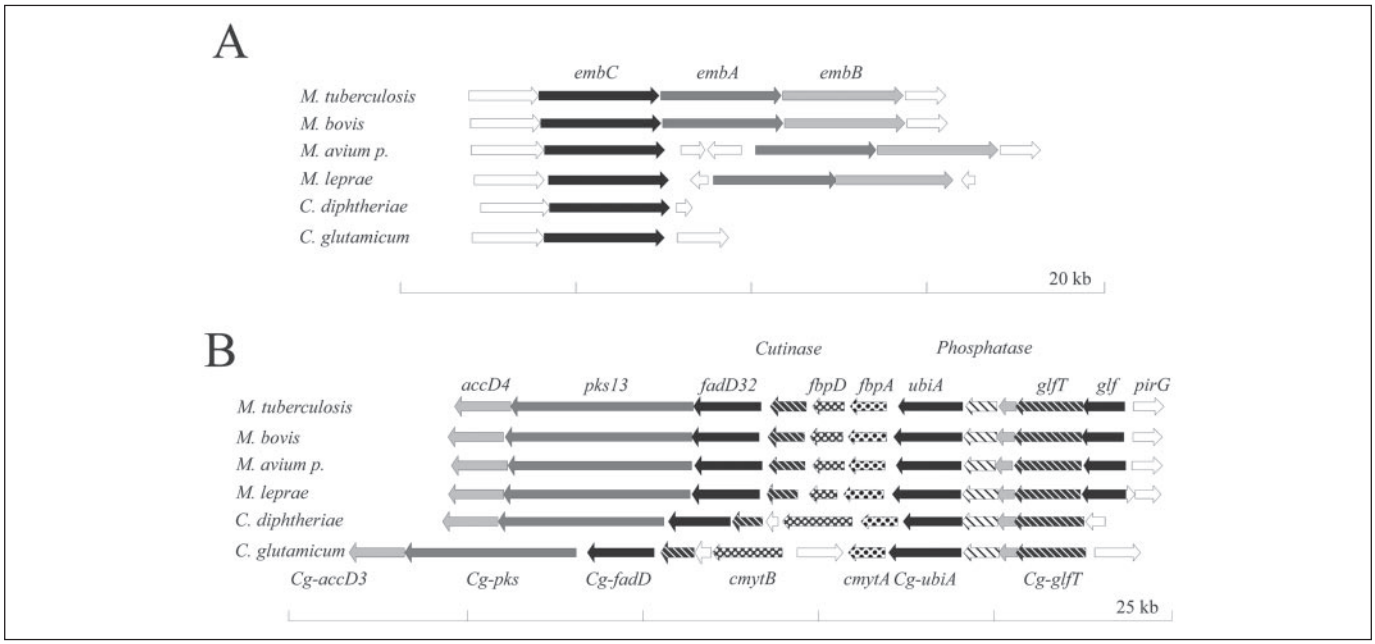

FIGURE 1. **Comparison of the mycolylarabinogalactan locus within the Corynebacterianeae.** *A*, the locus consists of *embC* with its upstream gene. *B*, the ten genes delimited by *glfT* and *accD4*. The open reading frames of *M. tuberculosis* shown in *panel A* cover the genome sequence from nucleotide 4,235,265 to 4,251,005, and in *panel B* from nucleotide 4,254,380 to 4,274,593, they are separated by fadE35 and a transposase (not shown). *M. avium p.*, *M. avium* subp. *paratuberculosis*.

prepared by bubbling HCl gas into ~2 ml of methanol until hot to the touch (~1 molar). The reagent (100 μl) was added to the per-*O*-methylated cell wall sample, and aliquots were analyzed by matrix-assisted laser desorption/ionization-time of flight mass spectrometry (MALDI-TOF MS) to monitor hydrolysis. The reaction was terminated by drying under nitrogen. MALDI-MS was performed using a PerSeptive Biosystems Voyager DE™ STR mass spectrometer (Applied Biosystems, CA) in the reflectron mode with delayed extraction. Samples were dissolved in methanol, and 1-μl aliquots were loaded onto a metal plate with 1 μl of the matrix 2,5-dihydrobenzoic acid. Sequazyme peptide mass standards were used as external calibrants (Applied Biosystems, CA).

GC and GC/MS of Sugar Composition and Sugar Linkage Analysis—Analysis of alditol acetate sugar derivatives was performed on a CE Instruments ThermoQuest Trace GC 2000. Samples were injected in the splitless mode. The column used was a DB225 (Supelco). The oven was programmed to hold at an isothermal temperature of 275 °C for a run time of 15 min. GC/MS was carried out on a Finnigan Polaris/GCQ Plus™. The column used was a BPX5 (Supelco).

RESULTS

Genome Comparison of the emb Locus—*M. tuberculosis*, *M. bovis*, *M. leprae*, and *M. avium* subsp. *paratuberculosis* have three *emb* genes (Fig. 1*A*), and at least one of these, *embB*, is suggested to be the target of EMB in mycobacteria (24, 32–34). However, *C. diphtheriae* and *C. glutamicum* have only one *emb* gene (35, 36). This is in accordance with the notion that the genome of *Corynebacterium* is considered to represent the archetype of Corynebacterianeae and has a low frequency of structural alterations and gene duplications (37). Interestingly, the single *emb* of *C. glutamicum*, *Cg-emb*, exhibits a higher identity to *embC* than to *embA* and *embB* of *Mycobacterium*, and increased expression of *Cg-emb* increases resistance of *C. glutamicum* toward EMB (38). In *M. leprae* and *M. avium* spp. *paratuberculosis* the paralogous *embAB* genes are separated by divergently transcribed genes that might indicate a more specific function and a separate regulation in these mycobacteria.

The above genomic comparison and the availability of the complete genome sequence of *C. glutamicum* has proven useful in the study of orthologous *M. tuberculosis* genes that are essential for viability. Therefore, in this study we examined the effects, in terms of arabinan biosynthesis and utilization of the sugar donor DPA, of firstly, Cg-*emb* by gene deletion in *C. glutamicum*, and secondly, disruption of *Cg-ubiA* (Fig. 1*B*), an enzyme recently shown to be involved in the biosynthesis of the sugar donor DPA.

*Construction of C. glutamicum*Δ*emb*—In our recent studies on *emb* of *C. glutamicum* we placed the chromosomally encoded gene under the control of a tetracycline repressor (38) and observed a number of physiological consequences, including reduced growth in presence of repressor (38). These studies encouraged us to test whether it would be possible to obtain a deletion of *emb* in *C. glutamicum*. The non-replicative plasmid pk19mobsacBΔ*emb* was constructed carrying sequences adjacent to *emb*. The vector was introduced into *C. glutamicum* and in several electroporation assays 3 kanamycin resistance clones were obtained, indicating integration of pk19mobsacBΔ*emb* into the genome by homologous recombination (Fig. 2, *A* and *B*). The *sacB* gene enables for positive selection of a second homologous recombination event that can result either in the original wild-type situation or in clones deleted of *emb*. More than 200 clones were obtained after 2–4 days and analyzed by PCR, but in all of them the wild-type situation was restored, illustrating a strong disadvantage of *emb* deletion. Only 3 clones appearing after 10 days were shown by PCR to have *emb* deleted. A further confirmation of *emb* deletion in one of the clones chosen was obtained in a Southern blot analysis (Fig. 2*C*). The chromosomal EcoRV fragment of the wild-type is 7.82 kb in size, whereas that of the *emb* deletion mutant is reduced to 4.35 kb, which mirrors the absence of *emb* of 3,438 bp. This confirms the integrity of the gene locus in the *emb* deletion mutant.

*In Vitro Growth Analysis of C. glutamicum*Δ*emb*—The deletion mutant was transformed with pEKEx2*emb* (38), and growth was studied on brain-heart-infusion media supplemented with sorbitol for osmotic stabilization (30). Whereas growth of *C. glutamicum* was completed after 8 h at an OD of 16, *C. glutamicum*Δ*emb* hardly reached an OD of 2 (Fig. 2*D*). However, complementation of the deletion mutant with pEKEx2*emb* restored the wild-type growth phenotype. mRNA transcript quantifications using LightCycler technology confirmed a 5-fold overexpression of *emb* due to pEKEx2*emb* when comparing expression of *emb* with its chromosomal copy (data not shown). *M. tuberculosis*

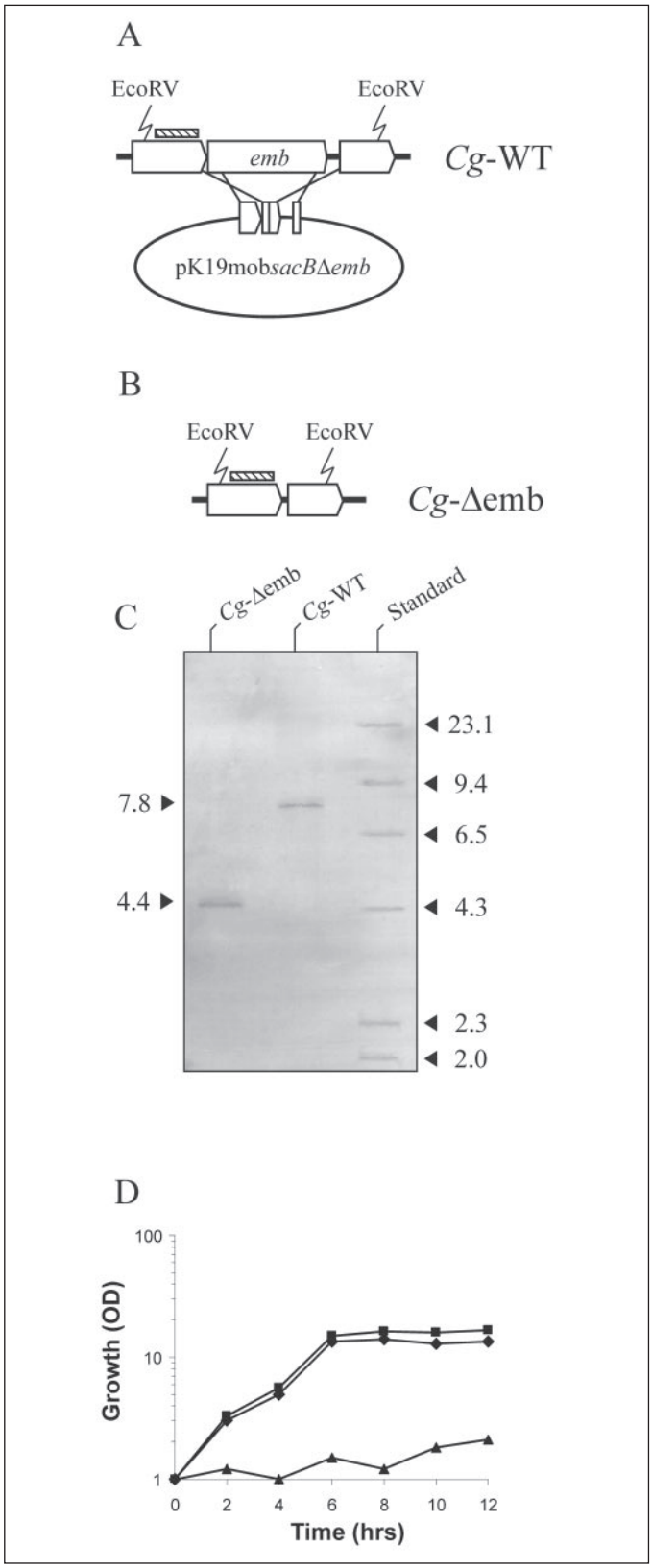

FIGURE 2. **Construction of *C. glutamicum*Δ*emb* mutant and growth analysis.** *A*, illustrated is *emb* with its adjacent genes of unknown function and the strategy to delete *emb* using the deletion vector pK19mob*sacB*Δ*emb*. The deletion vector carries 12 nucleotides of the 5′-end of *emb* and 12 nucleotides of its 3′-end thereby enabling the in-frame deletion of almost the entire *emb* gene. The *hatched small box* locates the probe used for the Southern blot analysis to detect hybridizing sequences on the 7.82-kb EcoRV fragment of the wild-type containing *emb*. Distances are not drawn to scale. *B*, situation of the original *emb* locus after deletion of *emb*, showing the intact organization of the originally adjacent genes in *C. glutamicum*Δ*emb* with the digoxigenin-labeled probe given as *hatched boxes* in *panels A* and *B*. *C*, final confirmation of the constructed strain via Southern blot analysis using chromosomal DNA from *C. glutamicum*Δ*emb* (*lane 1*), and Cg-WT (*C. glutamicum*) (*lane 2*). The *right lane* contains standards with their sizes given in kilobases. The *left lane* gives the sizes of the EcoRV fragments obtained from the wild-type, and the *emb* deletion mutant. The calculated sizes were 7.82 kb for the wild-type, and 4.35 kb for the deletion mutant. *D*, consequences of *emb* deletion on growth of *C. glutamicum* (■), *C. glutamicum* deleted of *emb* (*C. glutamicum*Δ*emb*, ▲), as well as the same strain expressing plasmid encoded *emb* (*C. glutamicum*Δ*emb* pEKEx2*emb* (♦).

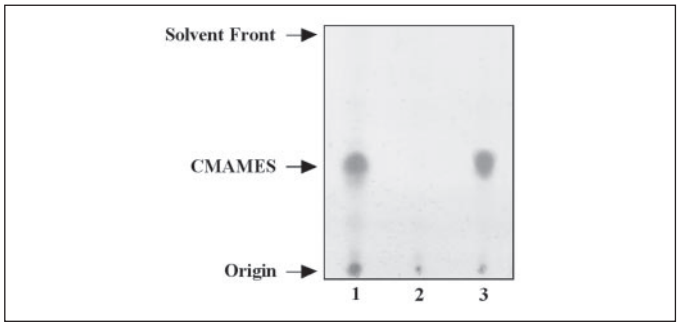

FIGURE 3. **Analysis of cell wall bound CMAMES from delipidated cells of *C. glutamicum*, *C. glutamicum*Δ*emb*, and *C. glutamicum*Δ*emb* pEKEx2*emb*.** *Lane 1*, *C. glutamicum*; *lane 2*, *C. glutamicum*Δ*emb*; and *lane 3*, *C. glutamicum*Δ*emb* pEKEx2*emb*. The bound corynomycolic acids from the delipidated extracts or purified cell walls were released by the addition of tetrabutylammonium hydroxide at 100 °C overnight and methylated as described under "Materials and Methods." An aliquot from each strain was subjected to TLC using silica gel plates (5735 Silica Gel $60F_{254}$, Merck), and developed in petroleum ether/acetone (95:5, v/v) and charred using 5% molybdophosphoric acid in ethanol at 100 °C to reveal CMAMES and compared with known standards (31).

embC, *embA*, and *embB* were cloned into pEKE2, however, although expression and sequence integrity of each clone was confirmed, no complementation of *C. glutamicum*Δ*emb* was achieved (data not shown). Analysis by light microscopy and electron micrographs showed that when compared with *C. glutamicum*, *C. glutamicum*Δ*emb* exhibited profound morphological changes similar to that of *C. glutamicum* treated with 100 μg/ml EMB (38) (data not shown).

Lipid Characterization of Mutants—To relate the phenotypic changes of the *C. glutamicum*Δ*emb* mutant to its cellular composition, the *C. glutamicum*Δ*emb* and its *Cg-emb* complemented strain along with *C. glutamicum* were analyzed for arabinogalactan-esterified corynomycolic acids. Bound lipids were analyzed by hydrolysis and the preparation of corynomycolic acid methyl esters (CMAMES). The profile of the extracted CMAMES is shown in Fig. 3. In the *C. glutamicum*Δ*emb* mutant, cell wall-bound corynomycolic acids were completely absent. The complementation of this strain with Cg-*emb* led to a restoration of cell wall-bound corynomycolic acids. These results suggest that Cg-*emb* is involved in arabinan biosynthesis of AG whereby deletion removes the sites of mycolylation (8).

*Glycosyl Compositional Analysis of Cell Walls from C. glutamicum, C. glutamicum*Δ*emb, and Cg-emb-complemented C. glutamicum*Δ*emb*—GC analysis of alditol acetates prepared from *C. glutamicum* cell walls (Fig. 4) reveals the presence of rhamnose (Rha), arabinose and galactose (Gal), respectively. Analysis of *M. tuberculosis* AG sugar composition shows that there are subtle differences when compared with *C. glutamicum*, with relatively reduced amounts of Rha (data not shown) (6, 7). Analysis of alditol acetates prepared from *C. glutamicum*Δ*emb* depicts a situation with a dramatically reduced (~90%), but not complete absence of arabinose content in the cell wall. It is also interesting to note that the relative amount of Rha is also reduced in this mutant. These results suggest that the presence of a high proportion of Rha in the cell walls of *C. glutamicum* is located or associated to the arabinan domains of the cell wall AG. Overall, these phenotypes are also observed upon treatment of *C. glutamicum* with 100 μg/ml of the anti-mycobacterial drug EMB (data not shown). Complementation of the emb mutant with plas-

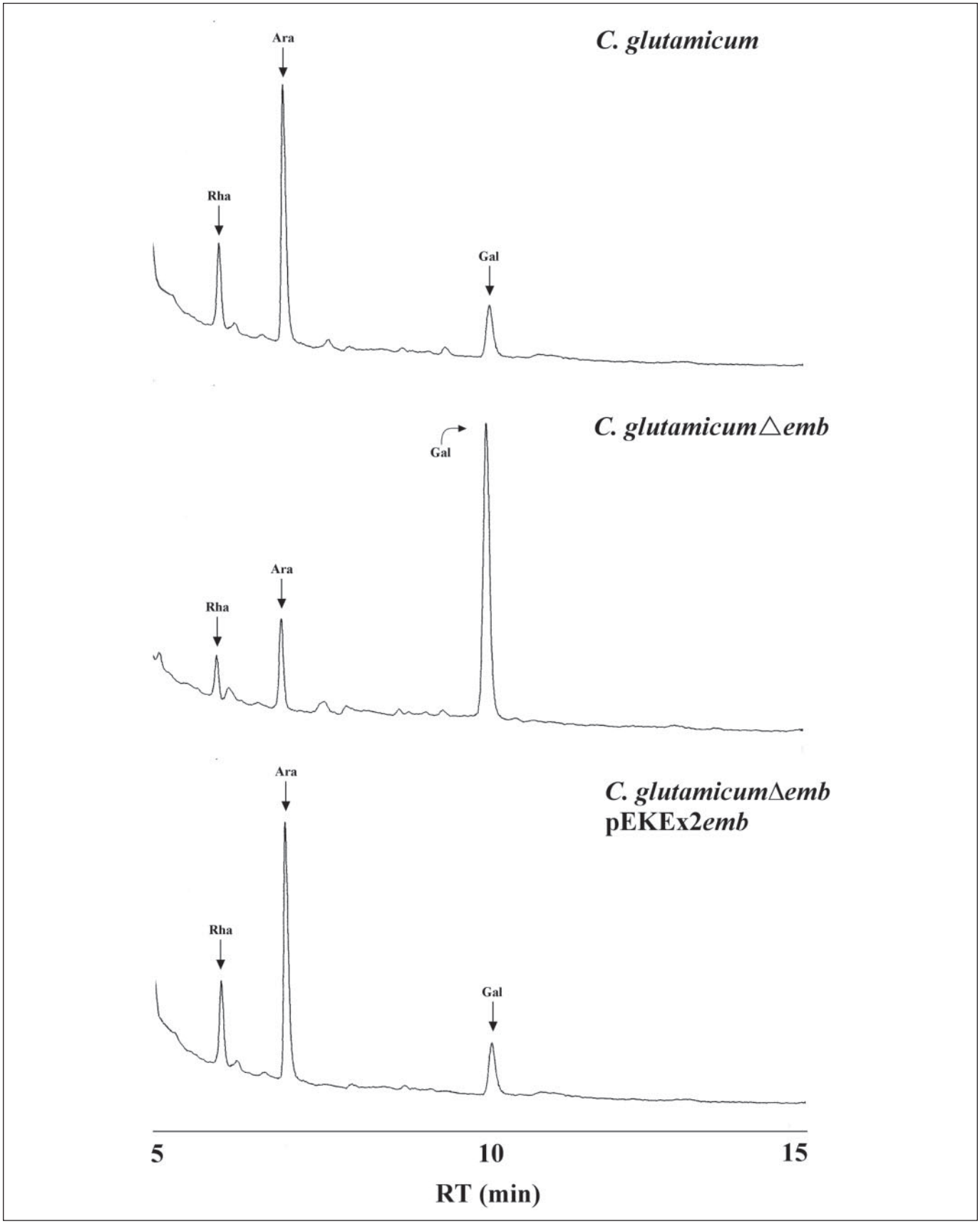

FIGURE 4. **Glycosyl compositional analysis of cell walls of *C. glutamicum*, *C. glutamicum*Δ*emb*, and *C. glutamicum*Δ*emb* pEKEx2*emb*.** Samples of purified cell walls were hydrolyzed with 2 M trifluoroacetic acid, reduced, per-*O*-acetylated, and subjected to GC as described under "Materials and Methods." Alditol acetate standards (Supelco) of Rha, Ara, and Gal were analyzed with retention times of 6, 7, and 10.1 min, respectively.

mid-encoded Cg-*emb* restored the glycosyl composition to that of *C. glutamicum* (Fig. 4).

Glycosyl Linkage Analysis of Cell Walls from C. glutamicum, C. glutamicumΔemb, and Cg-emb-complemented C. glutamicumΔemb—Per-*O*-methylated alditol acetate derivatives of *C. glutamicum*, *C. glutamicumΔemb*, and *C. glutamicumΔemb* complemented with plasmid-encoded *emb* are shown in Fig. 5. Glycosyl linkages present in *M. tuberculosis* (data not shown) and *C. glutamicum* include t-Ara*f*, 2-Ara*f*, 5-Ara*f*, 4-Rha*p*, t-Gal*f*, 3,5-Ara*f*, 5-Gal*f*, 6-Gal*f*, and 5,6-Gal*f*. The major difference between *C. glutamicum* and *M. tuberculosis* AG includes the presence of 2,5-Ara*f* and t-Rha*p* residues in *C. glutamicum*. In *C. glutamicumΔemb* a loss of 5-Ara*f*, 3,5-Ara*f*, 2,5-Ara*f*, and t-Rha*p* is observed with only t-Ara*f* residues appearing alongside 5-Gal*f*, 6-Gal*f*, and 5,6-Gal*f* residues. These results suggest that Cg-Emb actually plays a much larger role in the arabinosylation of AG in comparison to the results previously obtained with *M. smegmatis* EmbA and EmbB mutants (25), possibly suggesting some partial complementation of EmbA and EmbB in the singular *M. smegmatis emb* disruption mutants (25). In addition, the AG of *C. glutamicum* is unusual in that it would appear that the arabinan domains are also capped by t-Rha*p* residues, because these are absent in the *C. glutamicumΔemb* mutant. Complementation of the *emb* mutant with plasmid-encoded Cg-*emb* restored the glycosyl linkage profile to that of *C. glutamicum.* Glycosyl linkage analysis of *C. glutamicum* treated with 100 μg/ml of EMB yielded a CG/MS trace comparable to that of C. *glutamicumΔemb* (data not shown).

MALDI MS Analysis of Per-O-methylated Cell Walls from C. glutamicumΔemb—Cell walls derived from *C. glutamicumΔemb* were per-*O*-methylated and analyzed by MALDI-TOF MS, and the data are shown in Fig. 6*A*. The cluster of signals around *m/z* 4000 can be attributed to an AG polymer with truncated arabinan branching. The signals at *m/z* 3375, 3783, 4191, and 4599 are consistent with an AG glycan containing increasing numbers of Gal residues, $Ara_3Gal_{13}Rha$, $Ara_3Gal_{15}Rha$, $Ara_3Gal_{17}Rha$, and $Ara_3Gal_{19}Rha$, respectively. The additional signals observed can be assigned to AG glycans lacking an Ara or Rha residue, possibly resulting from the derivatization process. To define the Ara branching pattern on the galactan polymer, the per-*O*-methylated sample was subjected to time course methanolysis followed by re-methylation. The data generated (Fig. 6*B*) show numerous partial hydrolytic products affording informative ion series. A key region of the spectrum is shown expanded in Fig. 6*C*, and the assignment of significant products containing Rha are presented in TABLE ONE. Collectively, the data indicate that a linear galactan polymer extends from the reducing Rha and that the first Ara branch appears on the eighth Gal residue with further Ara branches appearing on the tenth and twelfth Gal residues. These results are supported by data generated from partial hydrolysis followed by per-*O*-deuteromethylation of the resulting hydrolytic products. The mass shifts observed resulting from per-*O*-deuteromethylation (data not shown) support the proposed Ara branching pattern.

MALDI MS analysis of per-*O*-methylated cell walls derived from *C. glutamicum* treated with 100 μg/ml EMB revealed a similar profile to that observed for cell walls derived from *C. glutamicumΔemb*. In addition, partial hydrolysis confirmed that *C. glutamicum* treated with EMB produced an AG, which had the same Ara branching pattern as described above in *C. glutamicumΔemb* (data not shown) illustrating the effects of EMB and *emb* deletion are super imposable.

Disruption of Cg-ubiA—We were intrigued by UbiA, a putative 4-hydroxybenzoate polyprenyltransferase and the possibility that UbiA was perhaps involved in DPA formation from 5-phosphoribofuranose pyrophosphate and decaprenol phosphate. The *ubiA* gene is present in

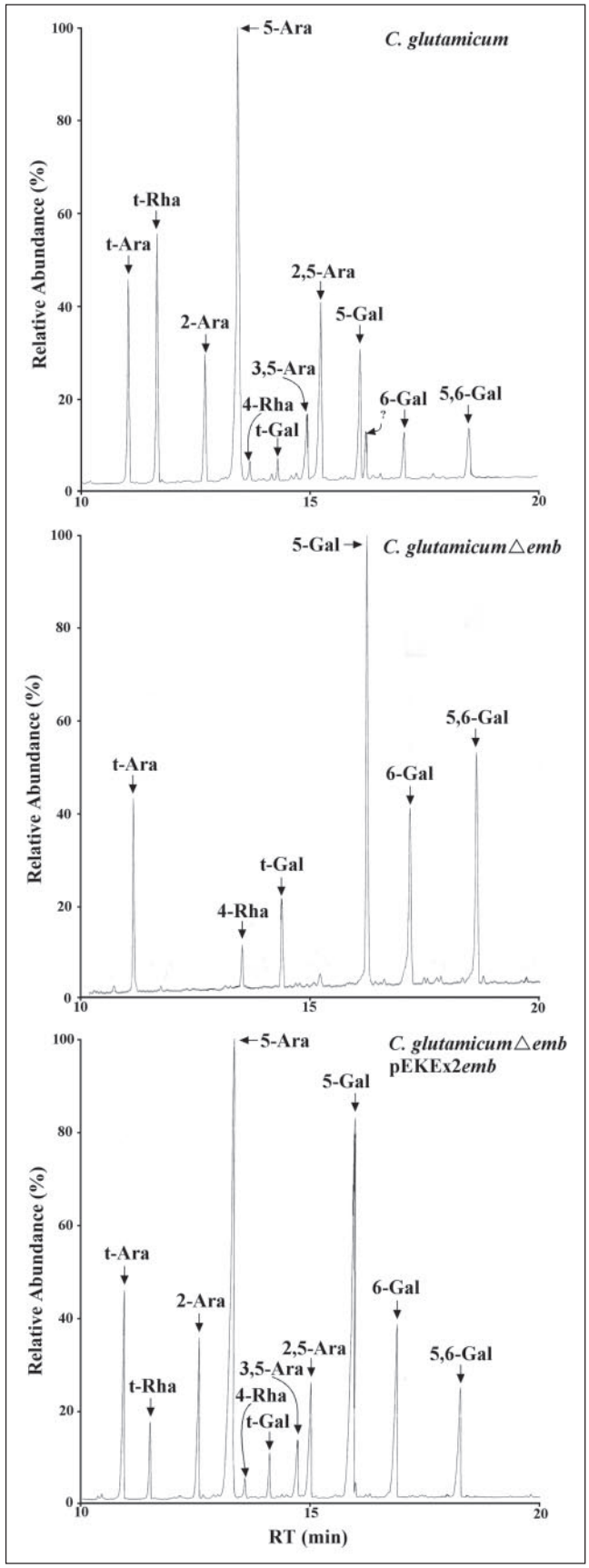

FIGURE 5. **Glycosyl linkage analysis of per-*O*-methylated cell walls prepared from *C. glutamicum*, *C. glutamicumΔemb*, and *C. glutamicumΔemb* pEKEx2*emb*.** Cell walls were prepared as described under "Materials and Methods" per-*O*-methylated, hydrolyzed, reduced, and per-*O*-acetylated. The resulting partially per-*O*-methylated, per-*O*-acetylated glycosyl derivatives were analyzed by GC/MS as described (6, 7).

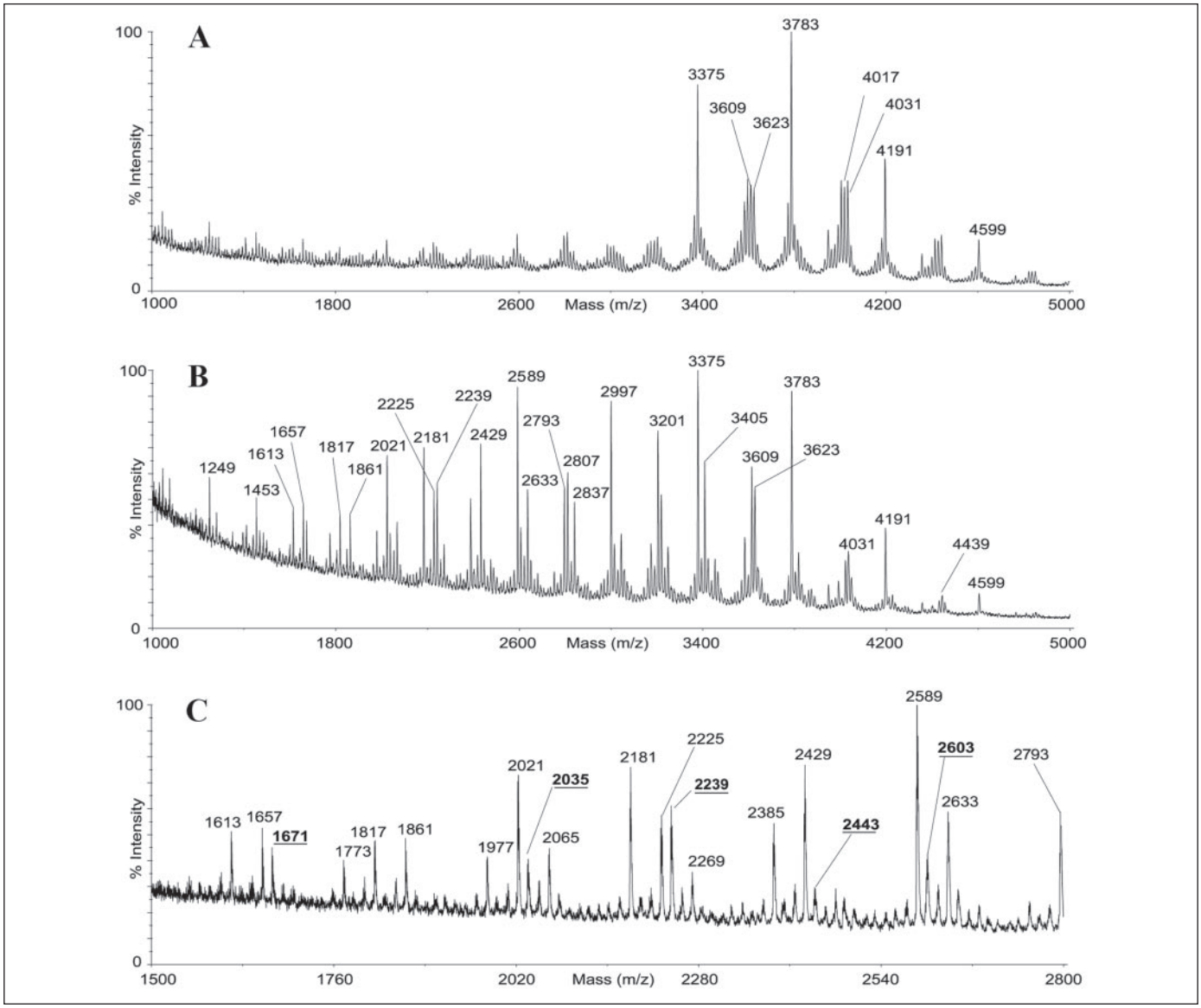

FIGURE 6. **MALDI-TOF MS of per-*O*-methylated cell walls derived from *C. glutamicum*Δ*emb*.** *A*, intact per-*O*-methylated cell walls. *B*, Per-*O*-methylated cell walls after partial hydrolysis with methanolic HCl followed by re-methylation. *C*, the key region of spectrum B expanded with salient signals *underlined*. Signal compositions are assigned in the text. The 100% Sep-Pak fractions are shown. All labeled signals are $[M+Na]^+$.

TABLE ONE

Assignment of the significant partial hydrolytic products detected by MALDI-TOF MS resulting from per-O-methylated cell walls derived from *C. glutamicum*Δ*emb*

m/z	Assignment[a]	*m/z*	Assignment[a]	*m/z*	Assignment[a]
1059	Gal_4Rha	2647	$AraGal_{11}Rha$	3375	$Ara_3Gal_{13}Rha$
1263	Gal_5Rha	2807	$Ara_2Gal_{11}Rha$	3419	$Ara_2Gal_{14}Rha$
1467	Gal_6Rha	2851	$AraGal_{12}Rha$	3463	$AraGal_{15}Rha$
1671	Gal_7Rha	3011	$Ara_2Gal_{12}Rha$	3579	$Ara_3Gal_{14}Rha$
2035	$AraGal_8Rha$	3055	$AraGal_{13}Rha$	3623	$Ara_2Gal_{15}Rha$
2239	$AraGal_9Rha$	3171	$Ara_3Gal_{12}Rha$	3783	$Ara_3Gal_{15}Rha$
2443	$AraGal_{10}Rha$	3215	$Ara_2Gal_{13}Rha$	4191	$Ara_3Gal_{17}Rha$
2603	$Ara_2Gal_{10}Rha$	3259	$AraGal_{14}Rha$	4599	$Ara_3Gal_{19}Rha$

[a] Assignment of Ara, Gal, and Rha based on their identification by linkage analysis.

Corynebacterianeae in synteny within the locus of other cell wall-related genes (Fig. 1*B*). The orthologue of *M. tuberculosis* Rv3806c in *C. glutamicum* is NCgl2781, and during compilation of this report was shown biochemically to perform the first step of DPA biosynthesis producing decaprenylphosphoryl-5-phosphoribose from 5-phosphoribofuranose pyrophosphate and decaprenol phosphate (39). To inactivate *ubiA* of *C. glutamicum*, plasmid pCg::*ubiA* was constructed and *C. glutamicum* transformed to kanamycin resistance. The resulting strain was confirmed by PCR analysis to have *ubiA* disrupted. This strain, *C. glutamicum*::*ubiA* was similar to *C. glutamicum*Δ*emb*, exhibited

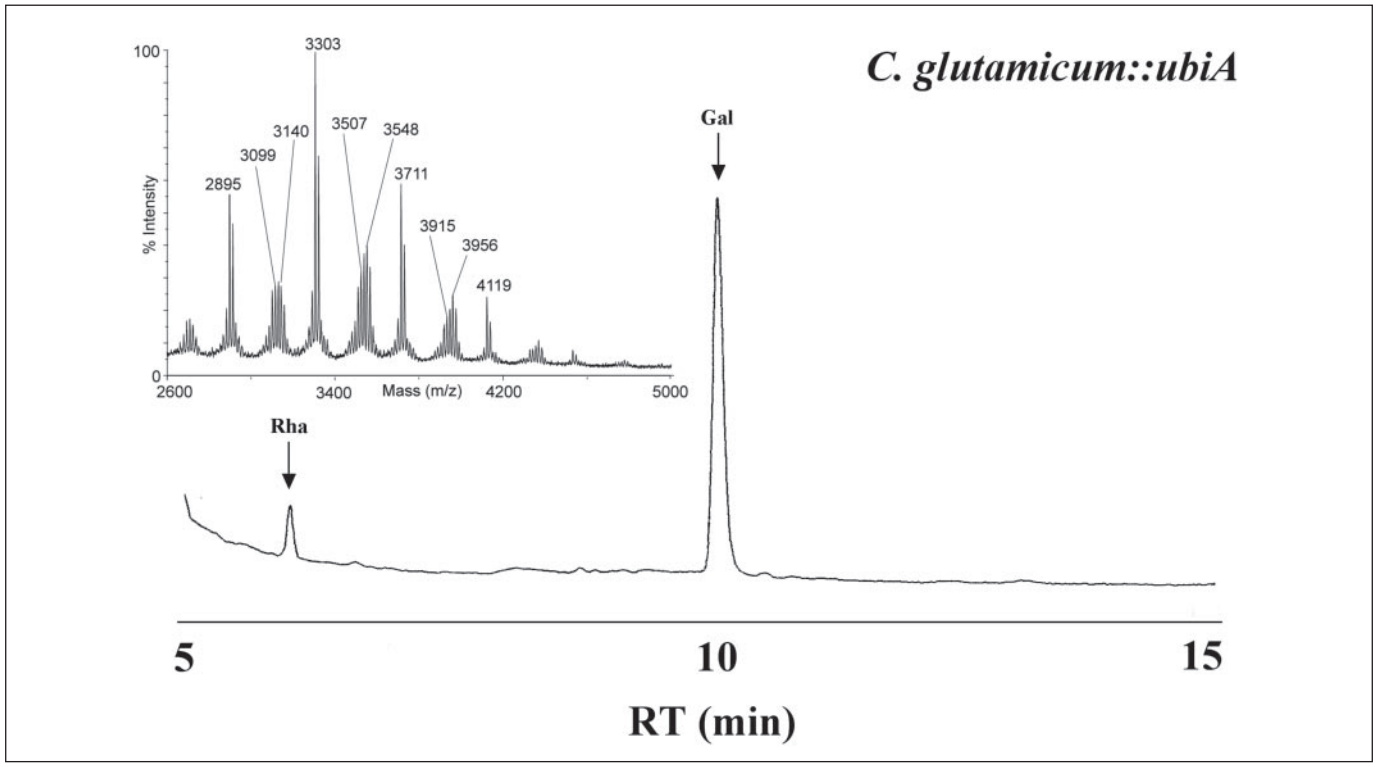

FIGURE 7. **Analysis of *C. glutamicum*::*ubiA* cell walls.** Samples of purified cell walls were hydrolyzed with 2 M trifluoroacetic acid, reduced, per-*O*-acetylated, and subjected to GC as described under "Materials and Methods" to provide glycosyl compositional analysis. The *inset* shows the MALDI-TOF MS of per-*O*-methylated cell walls derived from *C. glutamicum*::*ubiA*.

poor growth, and was devoid of bound cell wall corynomycolic acids (data not shown).

Glycosyl Compositional and MALDI MS Analysis of Cell Walls from C. glutamicum::ubiA—Interestingly, glycosyl compositional analysis of the resulting cell wall of *C. glutamicum::ubiA*, in contrast to *C. glutamicum*Δ*emb*, revealed a complete ablation of arabinan (Fig. 7). The results support a functional role of *Cg-ubiA* in cell wall arabinan biosynthesis (39) and demonstrate that DPA is the sole donor of Ara*f* residues in cell wall biosynthesis in Corynebacterianeae. Analysis of the per-*O*-methylated galactan derived form *C. glutamicum*::*ubiA* by MALDI MS revealed a cluster of signals consistent with a galactan backbone lacking any t-Ara residues as observed for the *emb* deletion mutant (see *inset*, Fig. 7). The signals at *m*/*z* 2895, 3303, 3711, and 4199 can be assigned the compositions $Gal_{13}Rha$, $Gal_{15}Rha$, $Gal_{17}Rha$, and $Gal_{19}Rha$, respectively. The additional signals observed can be assigned to galactan glycans lacking Rha or Gal, or retaining the GlcNAc attached to Rha.

DISCUSSION

The mAGP represents one of the most important cell wall components of members of the Corynebacterianeae, and it is essential for the viability of *M. tuberculosis* (27–29). It acts as a fulcrum between peptidoglycan and the impermeable hydrophobic mycolic acid layer. Furthermore, its biosynthesis is the target of the anti-mycobacterial drug EMB. However, the complete biosynthetic pathway and the cellular machinery involved in AG biosynthesis are still poorly understood (9).

As evident from the genome analyses (Fig. 1*A*) in *Mycobacterium* and *Corynebacterium* species analyzed to date, Cg-*emb* and its upstream region is strictly conserved, indicative of a core function common to all Corynebacterianeae and shown in this study to be involved in the majority of arabinan deposition in AG. Previous attempts to obtain *embA*, *embB*, and *embAB* deletion mutants in *M. tuberculosis* have been unsuccessful[2] and probably reflects the importance of AG in the cell wall ultrastructure of Mycobacterial species. However, individual disruptions of *embA* and *embB* in *M. smegmatis* have been obtained resulting in viable cells with observable phenotypic alterations to AG (25). The *embA* and *embB* mutants led to an alteration of the terminal Ara_6 motif of AG but still produced a highly arabinosylated AG polymer. The possibility existed that in either the *embA* or *embB* mutant partial complementation could ensue through the presence of either a functional copy of *embA* and *embB*, respectively, as gene duplication and redundancy appear common in *M. tuberculosis* (9, 25, 40). As a consequence the isolation of an arabinan-deficient cell wall mutant in *M. tuberculosis* appears fraught with difficulty.

With this in mind and because *C. glutamicum* possesses only a single *emb* gene, we attempted to construct an *emb* deletion mutant of *C. glutamicum*. The resultant deletion mutant produced a viable yet slow growing phenotype with profound morphological changes. Initial analysis of the corynomycolic acid content of *C. glutamicum*Δ*emb* showed that there was a complete absence of cell wall bound corynomycolates, hinting that there was a loss of corynomycolic acid esterification sites in the mutant, consistent with the loss of the terminal Ara_6 motif. Upon glycosyl compositional and linkage analysis, we observed in contrast to *M. smegmatis embA* and *embB* mutants (25) a 90% loss of cell wall arabinan, with all 5-Ara*f*, 3,5-Ara*f*, and 2,5-Ara*f* residues (also the capping t-Rha*p* residues) being absent in the cell wall of the *C. glu-tamicum*Δ*emb*, with the relative amounts of Gal unchanged. The minor amounts of Ara*f* residues were present as t-Ara*f* units. Furthermore, the AG derived from *C. glutamicum*Δ*emb* when analyzed by MALDI-TOF MS and partial acid hydrolysis indicated for the first time the location of the Ara branches of AG. A linear galactan extends from the reducing Rha and the first Ara branch appears on the eighth Gal residue with further Ara branches appearing on the tenth and twelfth Gal residues (Fig. 8). The observation of t-Ara*f* residues in

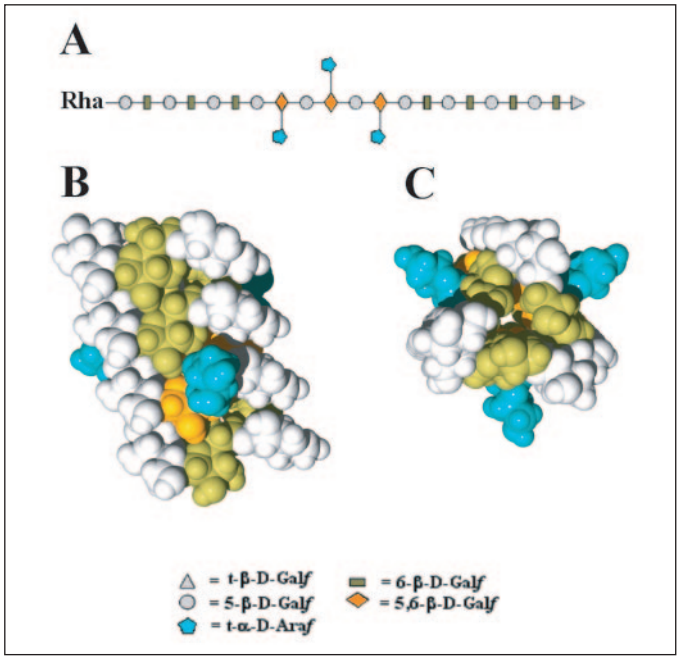

FIGURE 8. **Model representing truncated AG isolated from *C. glutamicum*Δ*emb* indicating the sites of arabinan attachment to the galactan moiety.** *A*, diagram representing the glycosidic linkages found in truncated AG isolated from *C. glutamicum*Δ*emb*, briefly, the linkages identified were t-Araf, 5-Galf, 6-Galf, 5,6-Galf, and t-Galf. *B*, space-filling representation of *C. glutamicum*Δ*emb* AG as viewed from side on (*perpendicular* to the peptidoglycan). *C*, as viewed from above, with the peptidoglycan being level with the plane of the page. The space-filled model of AG was prepared using SWEET (www.dkfz-heidelberg.de/spec/sweet2/doc/index.php), manipulated with SWISS PBD Viewer, and rendered with PovRay.

*C. glutamicum*Δ*emb* was somewhat surprising, because it has long been thought that the gene products of *embA* and *embB* in mycobacterial spp. are solely responsible for arabinan biosynthesis. Interestingly, the occurrence of arabinan deposition on an unaffected galactan backbone suggests that an unidentified arabinofuranosyltransferase might be responsible for the addition of the initial units onto the galactan domain. It is tempting to postulate that this hypothetical "priming enzyme" could fix the initial arabinan units onto the galactan chain for further elaboration by *emb* forming the fully matured AG. Interestingly, treatment of *C. glutamicum* with EMB results in a phenotype that is identical to the *C. glutamicum*Δ*emb*, with loss of esterified corynomycolic acids and a dramatically reduced arabinan content in AG. These results show that *emb* is indeed the target for EMB and that the arabinofuranosyltransferase activity of the "priming" enzyme remains unaffected. Given the importance of AG in *M. tuberculosis* viability and pathogenicity, it is tempting to suggest that this "priming" enzyme might be an ideal candidate to exploit as a drug target, because its disruption would result in a completely arabinan-deficient cell wall.

Due to the presence of t-Ara*f* residues in the *emb*-deleted strain of *C. glutamicum*, we endeavored to identify genes responsible for DPA biosynthesis, with the goal of deleting orthologues found in *C. glutamicum* for further phenotypic analysis. This was to rule out the possibility that the priming enzyme, unlike Emb, which utilizes DPA as a sugar donor, may use an alternative nucleotide sugar donor (41, 42).

Although the two gene loci depicted in Fig. 1 (*A* and *B*) are separated in *M. tuberculosis* by only two open reading frames (not shown), this part is not conserved and is at variance in *M. leprae* and other *Mycobacteria*. However, genes of the subsequent region extending from *accD4* to *glfT* are arranged in synteny in all Corynebacterianeae analyzed and are involved in some aspects of cell wall biosynthesis. For instance, *accD4* (*accD3* in *C. glutamicum*), which encodes the β-chain of an acyl carboxylase, which together with a second *accD* orthologue (*accD2* in *C. glutamicum* (31)) and the subsequent *pks13* and *fadD32*, make up the enzyme complex-activating (43) and -condensing (44) fatty acids, and these together form mycolic acids in a Claisen condensation reaction. Further upstream is the mycolyltransferase region (*fbpA* and *fbpC1* of *M. tuberculosis*), which is slightly different in *C. glutamicum* with one mycolyltransferase, *cmytB*, possessing a C-terminal extension (45, 46), and a transposase between the mycolyltransferases. *In silico* analysis of the region of genes, which have previously been shown to be involved in cell wall biosynthesis, resulted in the identification of a putative polyprenyltransferase, *ubiA*. The *ubiA* gene was found to reside in the genome of *C. glutamicum* adjacent to *glfT*, the gene responsible for galactan biosynthesis (Fig. 1*B*), and the region centered around *ubiA* is common to all Corynebacterianeae. *UbiA* is absent in Gram-negative bacteria and shares high homology with the *M. tuberculosis Rv3806c* of 53% identity, and interestingly, 49% identity with *noeC* of *Azorhizobium caulinodans* (47, 48). Recent studies have shown that UbiA is involved in the first step of DPA biosynthesis forming decaprenylphosphoryl-5-phosphoribose from 5-phosphoribofuranose pyrophosphate and decaprenol phosphate (39). Directly upstream of *ubiA* is a gene predicted to encode a phosphatase, which presumably dephosphorylates decaprenylphosphoryl-5-phosphoribose and then is converted to DPA via an epimerization process.[8] The generation of a *ubiA* mutant of *C. glutamicum* and chemical analysis of the purified cell wall revealed a complete loss of arabinan deposition and hence, a viable arabinan-deficient strain of *C. glutamicum*. As a result, we have presented unequivocal evidence that DPA is the only arabinan donor for AG biosynthesis ruling out the possibility of some other high energy arabinose nucleotide precursor. These studies also highlight UbiA as a possible drug target due to the lack of any other compensatory mechanisms to produce DPA and arabinan. As a result its disruption would result in a completely arabinan-deficient cell wall in Corynebacterianeae, such as *M. tuberculosis*.

In summary, because *C. glutamicum* and *M. tuberculosis* share a common cell wall ultrastructure and biosynthetic machinery, the deletion of *emb* and disruption of *ubiA* in *C. glutamicum*, has allowed us to shed further light on the role of these genes in cell wall AG biosynthesis in Corynebacterianeae such as *Mycobacterium* species.

Acknowledgment—We also thank Graham Burns for technical assistance.

REFERENCES

1. Bloom, B. R., and Murray, C. J. (1992) *Science* **257,** 1055–1064
2. Coyle, M. B., and Lipsky, B. A. (1990) *Clin. Microbiol. Rev.* **3,** 227–246
3. Funke, G., von Graevenitz, A., Clarridge, J. E., 3rd, and Bernard, K. A. (1997) *Clin. Microbiol. Rev.* **10,** 125–159
4. Sahm, H., Eggeling, L., and de Graaf, A. A. (2000) *Biol. Chem.* **381,** 899–910
5. McNeil, M., Daffe, M., and Brennan, P. J. (1990) *J. Biol. Chem.* **265,** 18200–18206
6. Besra, G. S., Khoo, K. H., McNeil, M. R., Dell, A., Morris, H. R., and Brennan, P. J. (1995) *Biochemistry* **34,** 4257–4266
7. Daffe, M., Brennan, P. J., and McNeil, M. (1990) *J. Biol. Chem.* **265,** 6734–6743
8. McNeil, M., Daffe, M., and Brennan, P. J. (1991) *J. Biol. Chem.* **266,** 13217–13223
9. Dover, L. G., Cerdeno-Tarraga, A. M., Pallen, M. J., Parkhill, J., and Besra, G. S. (2004) *FEMS Microbiol. Rev.* **28,** 225–250
10. Mikusova, K., Mikus, M., Besra, G. S., Hancock, I., and Brennan, P. J. (1996) *J. Biol. Chem.* **271,** 7820–7828
11. Mikusova, K., Yagi, T., Stern, R., McNeil, M. R., Besra, G. S., Crick, D. C., and Brennan, P. J. (2000) *J. Biol. Chem.* **275,** 33890–33897
12. Weston, A., Stern, R. J., Lee, R. E., Nassau, P. M., Monsey, D., Martin, S. L., Scherman, M. S., Besra, G. S., Duncan, K., and McNeil, M. R. (1997) *Tuber Lung Dis.* **78,** 123–131
13. Sanders, D. A., Staines, A. G., McMahon, S. A., McNeil, M. R., Whitfield, C., and Naismith, J. H. (2001) *Nat. Struct. Biol.* **8,** 858–863
14. Kremer, L., Dover, L. G., Morehouse, C., Hitchin, P., Everett, M., Morris, H. R., Dell, A., Brennan, P. J., McNeil, M. R., Flaherty, C., Duncan, K., and Besra, G. S. (2001) *J. Biol. Chem.* **276,** 26430–26440

[8] L. J. Alderwick, unpublished results.

15. Xin, Y., Lee, R. E., Scherman, M. S., Khoo, K. H., Besra, G. S., Brennan, P. J., and McNeil, M. (1997) *Biochim. Biophys. Acta* **1335,** 231–234
16. Wolucka, B. A., McNeil, M. R., de Hoffmann, E., Chojnacki, T., and Brennan, P. J. (1994) *J. Biol. Chem.* **269,** 23328–23335
17. Lee, R. E., Brennan, P. J., and Besra, G. S. (1997) *Glycobiology* **7,** 1121–1128
18. R. E. Lee, K. M., P. J. Brennan, G. S. Besra. (1995) *J. Am. Chem. Soc* **117,** 11829–11832
19. Hancock, I. C., Carman, S., Besra, G. S., Brennan, P. J., and Waite, E. (2002) *Microbiology* **148,** 3059–3067
20. Yagi, T., Mahapatra, S., Mikusova, K., Crick, D. C., and Brennan, P. J. (2003) *J. Biol. Chem.* **278,** 26497–26504
21. Takayama, K., Armstrong, E. L., Kunugi, K. A., and Kilburn, J. O. (1979) *Antimicrob. Agents Chemother.* **16,** 240–242
22. Takayama, K., and Kilburn, J. O. (1989) *Antimicrob. Agents Chemother.* **33,** 1493–1499
23. Belanger, A. E., Besra, G. S., Ford, M. E., Mikusova, K., Belisle, J. T., Brennan, P. J., and Inamine, J. M. (1996) *Proc. Natl. Acad. Sci. U. S. A.* **93,** 11919–11924
24. Telenti, A., Philipp, W. J., Sreevatsan, S., Bernasconi, C., Stockbauer, K. E., Wieles, B., Musser, J. M., and Jacobs, W. R., Jr. (1997) *Nat. Med.* **3,** 567–570
25. Escuyer, V. E., Lety, M. A., Torrelles, J. B., Khoo, K. H., Tang, J. B., Rithner, C. D., Frehel, C., McNeil, M. R., Brennan, P. J., and Chatterjee, D. (2001) *J. Biol. Chem.* **276,** 48854–48862
26. Zhang, N., Torrelles, J. B., McNeil, M. R., Escuyer, V. E., Khoo, K. H., Brennan, P. J., and Chatterjee, D. (2003) *Mol. Microbiol.* **50,** 69–76
27. Pan, F., Jackson, M., Ma, Y., and McNeil, M. (2001) *J. Bacteriol.* **183,** 3991–3998
28. Mills, J. A., Motichka, K., Jucker, M., Wu, H. P., Uhlik, B. C., Stern, R. J., Scherman, M. S., Vissa, V. D., Pan, F., Kundu, M., Ma, Y. F., and McNeil, M. (2004) *J. Biol. Chem.* **279,** 43540–43546
29. Vilcheze, C., Morbidoni, H. R., Weisbrod, T. R., Iwamoto, H., Kuo, M., Sacchettini, J. C., and Jacobs, W. R., Jr. (2000) *J. Bacteriol.* **182,** 4059–4067
30. Eggeling, L., and Bott, M. (2005) *Handbook of Corynebacterium glutamicum*, pp. 535–566, Taylor Francis Group, CRC Press, Boca Raton, FL
31. Gande, R., Gibson, K. J., Brown, A. K., Krumbach, K., Dover, L. G., Sahm, H., Shioyama, S., Oikawa, T., Besra, G. S., and Eggeling, L. (2004) *J. Biol. Chem.* **279,** 44847–44857
32. Ramaswamy, S. V., Amin, A. G., Goksel, S., Stager, C. E., Dou, S. J., El Sahly, H., Moghazeh, S. L., Kreiswirth, B. N., and Musser, J. M. (2000) *Antimicrob. Agents Chemother.* **44,** 326–336
33. Sreevatsan, S., Stockbauer, K. E., Pan, X., Kreiswirth, B. N., Moghazeh, S. L., Jacobs, W. R., Jr., Telenti, A., and Musser, J. M. (1997) *Antimicrob. Agents Chemother.* **41,** 1677–1681
34. Ramaswamy, S. V., Dou, S. J., Rendon, A., Yang, Z., Cave, M. D., and Graviss, E. A. (2004) *J. Med. Microbiol.* **53,** 107–113
35. Cerdeno-Tarraga, A. M., Efstratiou, A., Dover, L. G., Holden, M. T., Pallen, M., Bentley, S. D., Besra, G. S., Churcher, C., James, K. D., De Zoysa, A., Chillingworth, T., Cronin, A., Dowd, L., Feltwell, T., Hamlin, N., Holroyd, S., Jagels, K., Moule, S., Quail, M. A., Rabbinowitsch, E., Rutherford, K. M., Thomson, N. R., Unwin, L., Whitehead, S., Barrell, B. G., and Parkhill, J. (2003) *Nucleic Acids Res.* **31,** 6516–6523
36. Kalinowski, J., Bathe, B., Bartels, D., Bischoff, N., Bott, M., Burkovski, A., Dusch, N., Eggeling, L., Eikmanns, B. J., Gaigalat, L., Goesmann, A., Hartmann, M., Huthmacher, K., Kramer, R., Linke, B., McHardy, A. C., Meyer, F., Mockel, B., Pfefferle, W., Puhler, A., Rey, D. A., Ruckert, C., Rupp, O., Sahm, H., Wendisch, V. F., Wiegrabe, I., and Tauch, A. (2003) *J. Biotechnol.* **104,** 5–25
37. Nakamura, Y., Nishio, Y., Ikeo, K., and Gojobori, T. (2003) *Gene* (*Amst.*) **317,** 149–155
38. Radmacher, E., Stansen, K. C., Besra, G. S., Alderwick, L. J., Maughan, W. N., Hollweg, G., Sahm, H., Wendisch, V. F., and Eggeling, L. (2005) *Microbiology* **151,** 1359–1368
39. Huang, H., Scherman, M. S., D'Haeze, W., Vereecke, D., Holsters, M., Crick, D. C., and McNeil, M. R. (2005) *J. Biol. Chem.* **280,** 24539–24543
40. Belisle, J. T., Vissa, V. D., Sievert, T., Takayama, K., Brennan, P. J., and Besra, G. S. (1997) *Science* **276,** 1420–1422
41. Singh, S., and Hogan, S. E. (1994) *Microbios* **77,** 217–222
42. Klutts, J. S., Hatanaka, K., Pan, Y. T., and Elbein, A. D. (2002) *Arch. Biochem. Biophys.* **398,** 229–239
43. Trivedi, O. A., Arora, P., Vats, A., Ansari, M. Z., Tickoo, R., Sridharan, V., Mohanty, D., and Gokhale, R. S. (2005) *Mol. Cell* **17,** 631–643
44. Portevin, D., De Sousa-D'Auria, C., Houssin, C., Grimaldi, C., Chami, M., Daffe, M., and Guilhot, C. (2004) *Proc. Natl. Acad. Sci. U. S. A.* **101,** 314–319
45. Kacem, R., De Sousa-D'Auria, C., Tropis, M., Chami, M., Gounon, P., Leblon, G., Houssin, C., and Daffe, M. (2004) *Microbiology* **150,** 73–84
46. De Sousa-D'Auria, C., Kacem, R., Puech, V., Tropis, M., Leblon, G., Houssin, C., and Daffe, M. (2003) *FEMS Microbiol. Lett.* **224,** 35–44
47. Mergaert, P., D'Haeze, W., Fernandez-Lopez, M., Geelen, D., Goethals, K., Prome, J. C., Van Montagu, M., and Holsters, M. (1996) *Mol. Microbiol.* **21,** 409–419
48. Mergaert, P., Van Montagu, M., and Holsters, M. (1997) *Mol. Microbiol.* **25,** 811–817